Artesunate inhibits the growth of gastric cancer cells through the mechanism of promoting oncosis both *in vitro* and *in vivo*

Xiang Zhou[a], Wei-Jian Sun[a], Wei-Ming Wang[b], Ke Chen[a], Ji-Hang Zheng[a], Ming-Dong Lu[a], Pi-Hong Li[a] and Zhi-Qiang Zheng[a]

This study aims to investigate the significance and mechanism of artesunate involved in suppressing the proliferation of gastric cancer *in vitro* and *in vivo*. In the in-vitro experiments, artesunate inhibited the growth of gastric cancer cell lines (SGC-7901, BGC-823, and AGS) with concentration-dependent activity, with no significant effect on GES-1 cells. BGC-823 cells treated with artesunate showed the typical morphologic features of oncosis rather than apoptosis. Meanwhile, we observed calcium overload, downregulation of vascular endothelial growth factor expression, and upregulation of calpain-2 expression in the artesunate-treated BGC-823 cells. In addition, the in-vivo study showed that artesunate produced a dose-dependent tumor regression in nude mice. The antitumor activity of 240 mg/kg artesunate was similar to that of 10 mg/kg docetaxel. Furthermore, compared with the control group, no significant difference was observed in the body weight of artesunate-treated nude mice other than docetaxel-treated nude mice. These observations show that artesunate has concentration-dependent inhibitory activities against gastric cancer *in vitro* and *in vivo* by promoting cell oncosis through an impact of calcium, vascular endothelial growth factor, and calpain-2 expression. *Anti-Cancer Drugs* **24:920–927 © 2013 Wolters Kluwer Health | Lippincott Williams & Wilkins.**

Anti-Cancer Drugs 2013, **24**:920–927

Keywords: artesunate, calpain, gastric cancer, oncosis

[a]Department of Surgery, The Second Affiliated Hospital of Wenzhou Medical University and [b]Department of Surgery, The First Affiliated Hospital of Wenzhou Medical University, Wenzhou, People's Republic of China

Correspondence to Zhi-Qiang Zheng, Department of Surgery, The Second Affiliated Hospital of Wenzhou Medical University, 325027 Wenzhou, People's Republic of China
Tel: +86 13906652992; fax: +86 577 88653538;
e-mail: wzhealthwcw@aliyun.com

Received 21 May 2013 **Revised form accepted** 27 June 2013

Introduction

Artemisinin (ARS), also known as qinghaosu, is the active principle of the Chinese plant *Artemisia annua* L. (qinghao) used for more than 2000 years in Traditional Chinese Medicine (TCM) as a treatment remedy of malaria [1]. Several semisynthetic derivatives have been developed to increase the solubility of ARS in water, such as artemether, arteether, artesunate (ART), and others. Considerable evidence shows that ART is the most potent derivative *in vitro* [2]. Because of its lower side effects, ART has been used widely in the clinical practice of malarial patients [3]. Over the past 10 years, a growing body of evidence has showed that ART also has the characteristic of cytotoxicity against tumor cells *in vitro* and *in vivo*. Efferth *et al.* [4,5] have reported a profound cytotoxic action of ART against cancer cell lines of different tumor types, including leukemia, melanoma, the central nervous system, prostate carcinoma, and breast cancer. Further studies have shown that ART triggered apoptotic cell death in various tumor cell lines in both a p53-dependent and a p53-independent manner [6]. However, there is scarce research on the effect of ART on gastric cancer.

Recently, a few studies found an interesting phenomenon of oncosis cell death induced by ART that may be accompanied or not by apoptosis in several tumor cell lines, such as the human leukemia cell line [7] and pancreatic cancer [8]. Oncosis represents a novel cell death different from apoptosis [9]. Apoptosis is characterized by blebbing, cell shrinkage, nuclear fragmentation, chromatin condensation, chromosomal DNA fragmentation, and apoptotic bodies formation, whereas oncosis shows a lytic appearance of nuclei (karyolysis), swollen cytoplasm, completely disorganized structure of organelles, and ruptured membranes [9–11]. Currently, electron microscopy is the gold standard to identify apoptosis and oncosis.

In this study, we first evaluated the therapeutic effect of ART against gastric cancer cells *in vitro* and *in vivo*. The type of the cell death was assessed by electron microscopy and then the related pathways in ART-mediated cell death were examined.

Materials and methods

Reagents

ART was purchased from Guilin Pharmaceutical Co. Ltd. (Guangxi, China). Docetaxel was purchased from Sigma (St Louis, Missouri, USA). MTT [3-(4,5-dimethylthiazol-2-yl)-2,5-diphenyltetrazolium bromide] and Ca^{2+} dye Fluo-3/AM were purchased from Beyotime (Haimen, China). The annexin V-FTIC kit was purchased from Keygen Biotech (Nanjing, China). Rabbit anti-human vascular endothelial growth factor (VEGF) and rabbit

0959-4973 © 2013 Wolters Kluwer Health | Lippincott Williams & Wilkins DOI: 10.1097/CAD.0b013e328364a109

anti-human calpain-2 polyclonal antibody were purchased from Abcam (Cambridge, UK).

Cell lines and culture

Human gastric cancer cell lines SGC-7901, BGC-823, and AGS were obtained from the cell resource center of the Shanghai Biological Sciences Institute (Chinese Academy of Sciences, Shanghai, China). GES-1 (human gastric mucosal epithelial cell line), purchased from Beijing Institute for Cancer Research (Beijing, China), was used as a normal cell model to examine the nonspecific cytotoxicity of the drug tested. SGC-7901 and BGC-823 cells were maintained in RMPI1640 (Beyotime), the AGS cells were grown in DMEM/F12 (1 : 1) (Beyotime), and GES-1 cells were cultured in DMEM (Beyotime). All media were supplemented with 10% fetal bovine serum (Invitrogen, Carlsbad, California, USA), 100 U/ml penicillin (Beyotime), and 100 μg/ml streptomycin (Beyotime). The cultures were incubated at 37°C in a humidified atmosphere of 5% CO_2.

Mice

Male BALB/c athymic nude mice (5 weeks old) were purchased from Shanghai Slac Laboratory Animal Co. Ltd (Shanghai, China). The protocol for the animal experiment was approved by the Institutional Animal Committee of Wenzhou Medical College. All animals received care in accordance to the 'Guide for the Care and Use of Laboratory Animals', Permit Number: SYXK (zhe) 2010-0150.

MTT cell viability assay

Cells (1×10^4) were plated in 96-well plates (Falcon; Becton Dickinson, Franklin Lakes, New Jersey, USA) and cultured in a humidified incubator (at 37°C with 5% CO_2 and 95% air) for adhesion overnight. They were then separately exposed to various concentrations of ART (16.25, 32.5, 65, 130, 260 μmol/l) for 48 h, each in sextuplicate. Following the incubation, 20 μl of MTT solution was added. The culture was then incubated for 4 h to convert MTT into formazan. Thereafter, the supernatant was discarded and 150 μl of dimethylsulfoxide (DMSO) was added to dissolve the formazan. The absorbance was measured at a wavelength of 490 nm. The sensitivity of cells to ART was measured by IC_{50} (IC_{50} values defined as the concentration inducing 50% loss of cell viability).

Electron microscopy

Cells were fixed with 2.5% (v/v) glutaraldehyde in 0.1 mol/l PBS (pH 7.4) for 2 h, washed with PBS twice, and postfixed in 0.01 g/ml osmium tetroxide for 1 h. The cells were dehydrated in acetone and embedded in epoxy resin. Ultrathin sections were stained with uranyl acetate and lead citrate, and examined under a transmission electron microscope (Hitachi H-7500; Hitachi, Tokyo, Japan).

Annexin V-FITC/PI staining experiment

Quantification of oncosis cells was performed using the Annexin V-FITC/PI detection kit (Keygen Biotech). BGC-823 cells were treated with different concentrations of ART (0, 32.5, 65, 130 μmol/l) for 24 h at 37°C. Cells (5×10^5) were collected, washed twice with PBS, and suspended in 500 μl binding buffer. Subsequently, 5 μl AnnexinV-FITC and 5 μl PI were added and incubated for 5–15 min at room temperature, with protection from light. Detection of viable cells (AnnexinV-FITC-negative, PI-negative), early apoptotic cells (AnnexinV-FITC-positive, PI-negative), and oncosis necrosis cells (AnnexinV-FITC-positive, PI-positive) was performed using a FACSCalibur (Becton Dickinson).

Measurement of cytosolic Ca^{2+}

Intracellular Ca^{2+} levels were determined with the Ca^{2+}-sensitive fluorochrome Fluo-3/acetoxymethyl ester (Fluo-3/AM) using a Becton Dickinson FACS Caliber flow cytometer [12]. Cells were incubated with 3 μmol/l Fluo-3/AM at 37°C for 30 min in the dark after the treatment with ART as described above. Cells were then gently rinsed three times with D-Hanks' solution and the fluorescence was analyzed by flow cytometry. Fluo-3/AM binds cytoplasmic free calcium and emits a green fluorescence (peak at 526 nm) detected in the fluorescence channel FL-1, with excitation at 488 nm and emission at 530 nm.

Immunocytochemistry

BGC-823 cells grown as a monolayer on a slide were treated with or without ART (65 μmol/l) for 24 h. Then, they were fixed with fresh paraformaldehyde (4%). Afterwards, they were permeabilized with 0.3% Triton X-100 in PBS, blocked for endogenous peroxidase by 3% hydrogen peroxide, and for nonspecific binding sites by 5% goat serum. The slides were incubated for 18 h at 4°C with the appropriate dilution (1 : 100) of polyclonal rabbit anti-human VEGF and calpain-2 antibody. Samples were then incubated for 30 min at room temperature with the appropriate dilution (1 : 100) of HRP-IgG goat anti-rabbit antibody. The slides were colored with 3,3′-diaminobenzidine (DAB) and Mayer's hematoxylin, used for counterstaining, and were then dehydrated and coverslipped. The positive cells of VEGF and calpain-2 protein were brown yellow in the cytoplasm.

Western blot analysis

After treatment with ART for 24 h, cells were suspended in 100 μl of ice-cold RIPA lysis buffer and incubated at 4°C for 1 h. The extracts were cleared by centrifugation at 12 000 rpm for 20 min at 4°C and the protein content was quantified using a bicinchoninic acid (BCA) protein assay kit (Pierce, Rockford, Illinois, USA) according to the manufacturer's instructions. Thirty micrograms of protein was separated on a 10% SDS-PAGE gel and transferred to polyvinylidene difluoride (PVDF) membranes. The blots

were blocked with 0.05 g/ml nonfat dry milk, incubated with primary antibody overnight at 4°C, and then incubated with HRP-conjugated secondary antibody for 1 h at room temperature. Immunoreactive proteins were detected by enhanced chemiluminescence (Amersham Biosciences, Piscataway, New Jersey, USA).

In-vivo therapeutic efficacy in established tumors

We injected 1×10^7 BGC-823 cells subcutaneously into each anterior flank region of nude mice. Treatment was started when the injected cell mass reached a mean volume of 200 mm^3. After the tumor established, the mice were randomized into five groups ($n = 5$ per group) and saline was administered only in the untreated control group, docetaxel (10 mg/kg/day, intraperitoneally every 3 days) in the chemotherapy control group, or ART (60, 120, or 240 mg/kg/day, intraperitoneally every day). The mice were killed and the tumors were excised after 15 days of treatment. The greatest tumor dimensions were measured serially with calipers and tumor volume was calculated using the following formula: tumor volume (mm^3) = (width^2 × length)/2 [13].

Statistical analysis

All quantitative assays were carried out in triplicate. The results are expressed as mean ± SD. The statistical significance was evaluated by one-way analysis of variance, followed by least significant difference or Dunnett's T3 test. Statistical significance was considered at a P value less than 0.05.

Results

ART inhibited gastric cancer cells proliferation *in vitro*

The dose-dependent cell proliferation curves showed that ART exerted cytotoxicity in all gastric cell lines examined (SGC-7901, BGC-823, and AGS) in a micromolar dose range (Fig. 1). The IC_{50} values of ART against SGC-7901, BGC-823, and AGS cells were 78.2, 72.3, and 102.3 μmol/l, respectively. Cytotoxic activities of ART against gastric cancer cells were about 2.2–5.2 times more than that of the normal human gastric mucosal epithelial cell line (GES-1) (IC_{50} = 375.0 μmol/l), indicating that ART showed selective cytotoxicity in human gastric cancer cells.

ART-induced cell death had ultrastructural features of oncosis

Electron microscopy showed that the control BGC-823 cells had intact cellular morphology with normal nuclei and organelles (Fig. 2a and b). In contrast, BGC-823 cells treated with 65 μmol/l ART for 48 h showed a swollen cytoplasm, completely disorganized structure of organelles, and numerous small and large cytoplasmic vacuoles. The most prominent nuclear changes were dilation of the nuclei and irregular clumping of chromatin (Fig. 2c). High-magnification electron micrographs of ART-treated BGC-823 cells showed severely damaged swollen organelle (Fig. 2d). These morphologic features were consistent with a type of cell death called oncosis [9,11].

Fig. 1

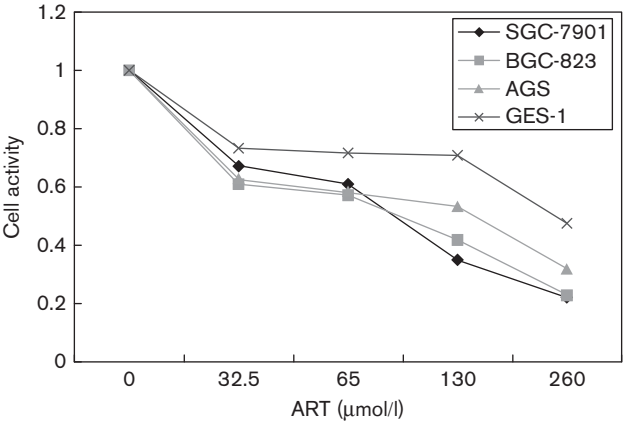

Cytotoxic effects of artesunate (ART) on human gastric cancer cells. SGC-7901, BGC-823, AGS, and normal gastric mucosal epithelial cell line (GES-1) were treated with the indicated concentrations of ART for 48 h. Mean values for three independent cell viability MTT assays were plotted.

Assessment of oncosis in BGC-823 cells

Apoptotic cells can be differentiated from oncotic cells using a double-staining technique with annexin V and propidium iodide as the latter does not penetrate cells with an intact cell membrane [14]. Using this technique, early apoptotic cells are only colored by annexin V, whereas oncotic cells are stained with both annexin V and propidium iodide [14]. As shown in Fig. 3a, in the early stage, the number of oncotic cells increased accompanied by an increase in the drug concentration and the apoptotic cells were rarely found in all groups. The oncotic index of BGC-823 cells in different groups was statistically significantly different ($P < 0.001$) (Fig. 3b).

Ca^{2+} was involved in ART-induced BGC-823 cell oncosis

To examine whether ART-induced oncosis was associated with increased cytosolic Ca^{2+}, we evaluated the intensity of cytosolic Fluo-3 fluorescence, an indicator of cytosolic Ca^{2+} in BGC-823 cells treated with or without ART. Following treatment with different concentrations of ART (0, 32.5, 65, 130 μmol/l) for 24 h, cytosolic Ca^{2+} was 2.4–3.2 times higher than that in the control group (Fig. 4). Thus, ART caused a transient and sustained increase in cytosolic Ca^{2+} compared with the control group.

Effect of ART on VEGF and calpain-2 protein expression in BGC-823 cells

To investigate the mechanism by which ART induces oncosis, we analyzed the expression of oncosis-associated

Fig. 2

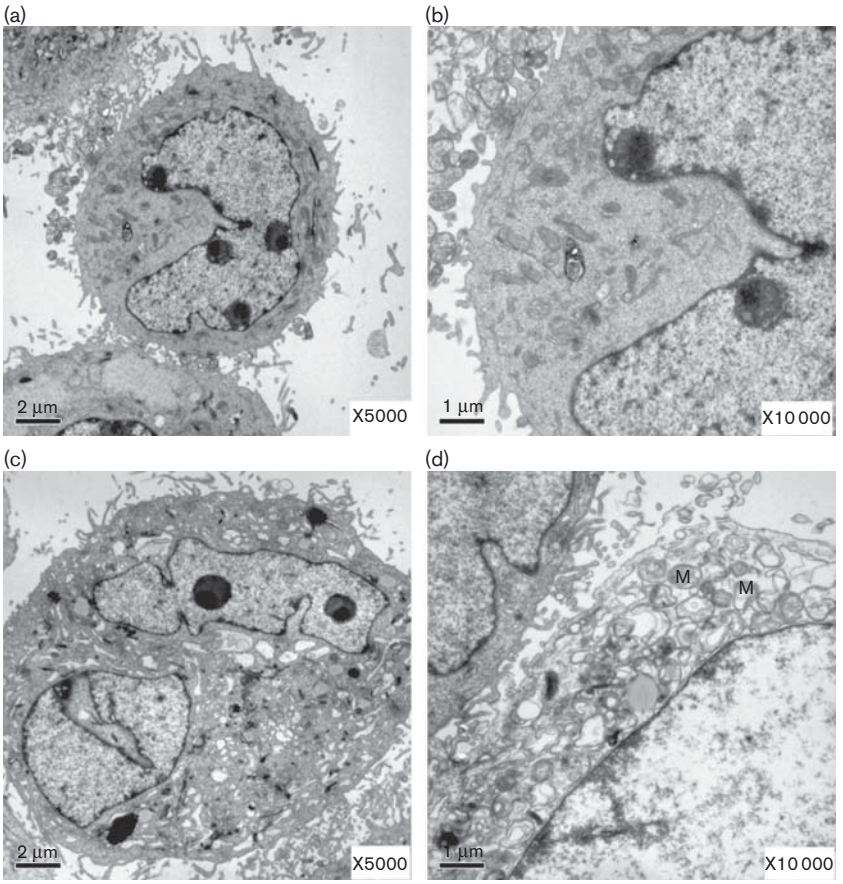

Artesunate (ART)-mediated cell death. (a) Untreated control BGC-823 cell. (b) High-magnification electron micrograph showing a disperse pattern of chromatin configuration and a prominent nucleolus. The cytoplasm shows abundant mitochondria. (c) Disruption of the nuclear and cytoplasmic organization by ART. (d) High-magnification electron micrograph showing the cytoplasmic swelling, the dilation of the ER elements, swollen mitochondria (M), and ruptured plasma membrane late in the process of ART-treated cell death.

protein in BGC-823 cells using immunohistochemical and western blot analysis. As shown in Fig. 5, compared with the negative control group, there was a marked decrease in VEGF expression and a significant increase in calpain-2 expression in ART (65 μmol/l)-treated cells.

ART inhibited the proliferation of gastric cancer cells *in vivo*

ART induced a dose-dependent suppression of BGC-823 tumor growth in nude mice. At the end of the study (day 15), daily administration of 60, 120, and 240 mg/kg ART (intraperitoneally) in the established BGC-823 xenografts mode (average tumor volume = 200 mm^3) inhibited tumor growth by 37, 45, and 58%, respectively ($P < 0.001$ vs. saline controls). Docetaxel (10 mg/kg/day, intraperitoneally every 3 days) reduced tumor growth by 55% on day 15, which did not differ significantly from the result obtained with 240 mg/kg ART (Fig. 6b).

ART-treated and control mice did not show any evidence of significant side effects and their body weights did not differ from each other. In contrast, there was a 23% reduction in body weight in docetaxel-treated mice (Fig. 6c). In addition, mice treated with docetaxel were weak and inactive, and two of them died on day 15.

Discussion

Most chemotherapy drugs have extensive side effects and produce multidrug resistance in some cases, particularly, cisplatin and fluorouracil [15]. ART has been used to treat multidrug-resistant malaria safely, confirmed to be effective on a number of human cancer cell line types in culture as well as in certain animal models recently [8,16–19]. In this study, the anticancer effects of ART on human gastric cancer cells were evaluated both *in vitro* and *in vivo*. The results of the in-vitro study showed that ART exerted a high growth-inhibitory action ($P < 0.01$) on various human gastric cancer cell lines, but exerted a less cytotoxic effect on normal GES-1 cells. The in-vivo antitumor activity of ART was similar to that of docetaxel. Furthermore, compared with the control group, no significant difference was observed in the body

Fig. 3

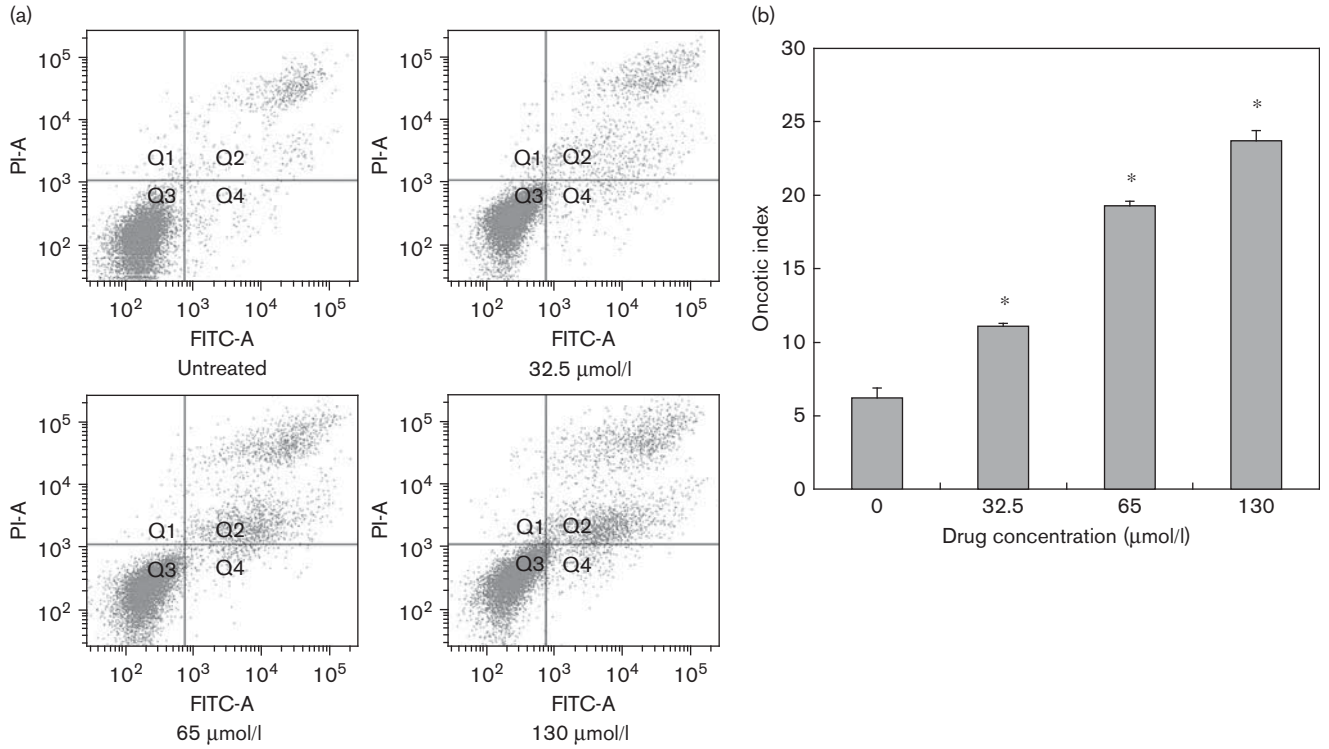

Assessment of oncosis of BGC-823 cells. (a) Flow cytometric analysis of early stage of artesunate-treated BGC-823 cells stained with annexin V-FITC and PI. Apoptotic cells are presented in the right-lower quadrant of the figure (Q4), oncotic cells in the right-upper quadrant (Q2), living cells in the left-lower quadrant (Q3), and cell debris in the left-upper quadrant (Q1). (b) Analytical data show the oncotic index of BGC-823 cells in different groups. Each experiment was conducted three times. *$P<0.001$, compared with the control.

Fig. 4

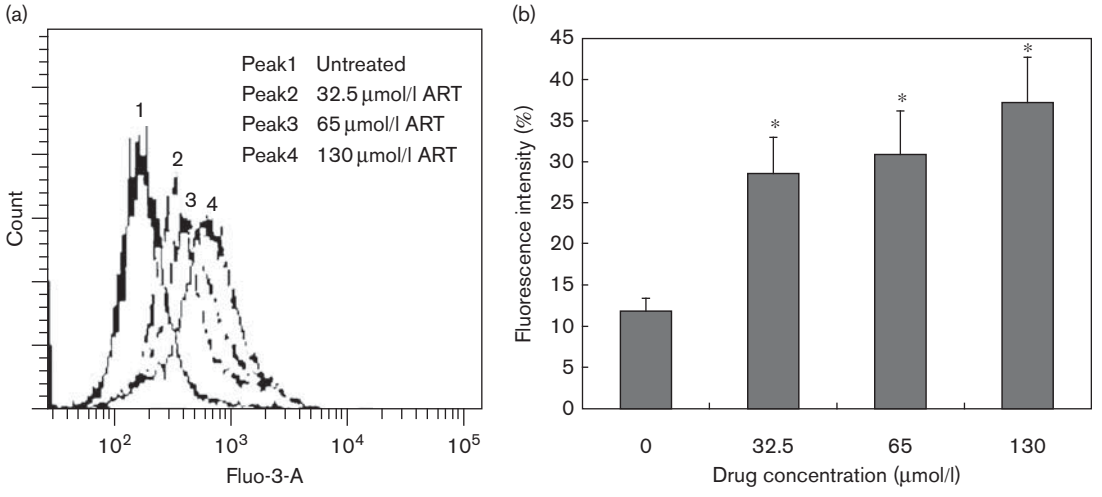

Ca^{2+} was involved in BGC-823 cell oncosis induced by artesunate (ART). (a) Concentration–course effect of ART (24 h) on cytosolic Ca^{2+} in BGC-823 cells after treatment for 0, 32.5, 65, and 130 μmol/l. Cells loaded with Fluo-3/AM (3 μmol/l; Fluo-3-A) were measured by flow cytometry. (b) Each experiment was conducted in triplicate and the data represent the mean±SD. *$P<0.001$, compared with the control.

Fig. 5

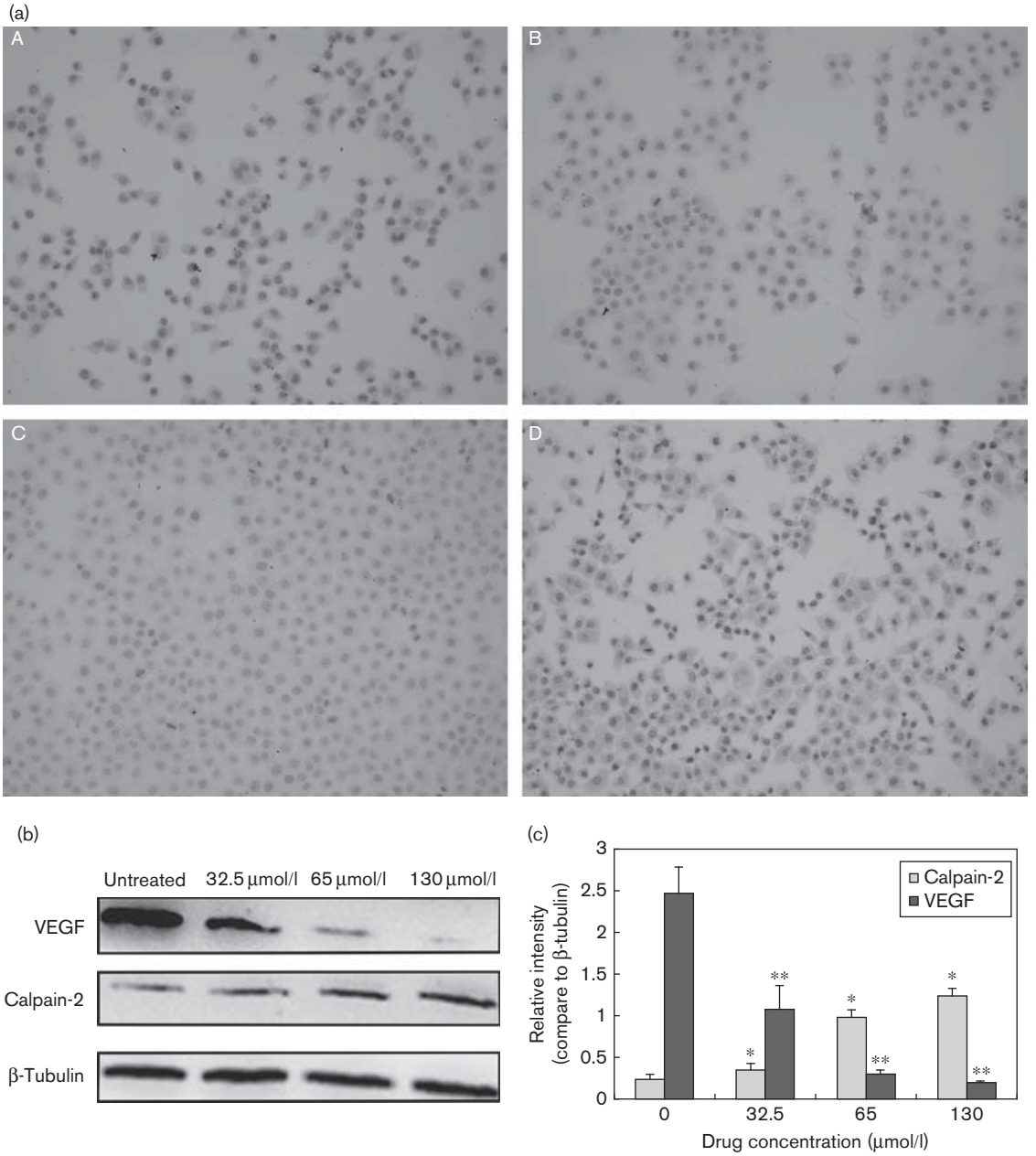

Effects of artesunate (ART) on VEGF and calpain-2 protein expression of BGC-823 cells. (a) A, Vascular endothelial growth factor (VEGF) expression in the control group; B, VEGF expression in the 65 μmol/l ART-treated group; BGC-823 cells expressed VEGF protein. ART downregulated VEGF expression; C, calpain-2 expression in the control group; D, calpain-2 expression in the 65 μmol/l ART-treated group (light microscope, S-P technique of immunocytochemistry, stained with hematoxylin again, × 200). ART upregulated calpain-2 expression. (b) Cells were treated with ART at different concentrations and 30 μg protein was separated on a 10% SDS-PAGE gel. β-Tubulin was used as an internal standard to normalize loadings. (c) Relative expression levels of VEGF and calpain-2 were expressed as the relative intensity compared with β-tubulin. Values are the mean±SD of data from three independent experiments. $^{*}P<0.05$, $^{**}P<0.001$ compared with the control.

weight of ART-treated nude mice other than docetaxel-treated nude mice, which suggested that ART efficiently retards tumor growth in nude mice without apparent toxicity to the hosts. Thus, ART has the potential to be developed as a new chemotherapy agent against gastric cancer.

Researchers have found that two different morphological changes exist in the antitumor effect of ART: cell pyknosis and cell swelling. Majno and Joris named these patterns apoptosis and oncosis, respectively, which are also considered to be two different modes of cell death [9,11]. Currently, electron microscopy is the gold

Fig. 6

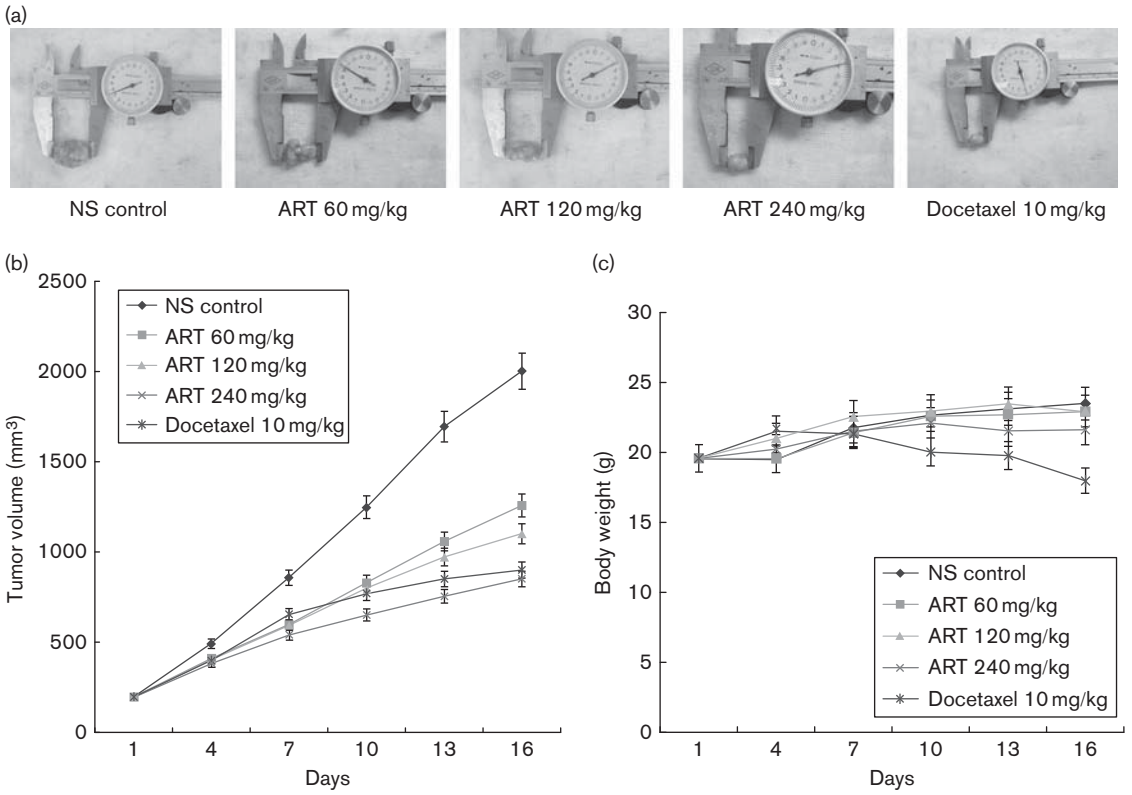

Antitumor activity of artesunate (ART) in nude mice. (a) Photographs of subcutaneously implanted gastric tumors on day 15 of treatment. 240 mg/kg ART and 10 mg/kg docetaxel significantly inhibited tumor growth. (b) ART (60, 120, or 240 mg/kg), docetaxel (10 mg/kg), or saline ($n=5$ per group) was administered intraperitoneally when BGC-823 cell tumors (subcutaneously in the flank) reached an average volume of 200 mm^3. Semiweekly assessment of tumor volume showed that administration of ART inhibited BGC-823 tumor growth in nude mice. (c) The body weights of the ART-treated mice were indistinguishable from those of saline controls ($P<0.802$), whereas docetaxel treatment reduced body weight ($P<0.001$).

standard to identify oncosis, whereas it is widely recognized that AnnexinV-FITC and PI double staining is the best method for assessment oncosis [14]. We used electron microscopy to observe the morphology of ART-treated cell death. It showed cytoplasmic swelling, dilation of the ER elements, swollen mitochondria (M), and ultimately ruptured plasma membrane, which were typical morphologic characteristics of oncosis-like cell death. Furthermore, oncosis-like cell death has an early ruptured plasma membrane and has an increased permeability of PI, which is used to distinguish apoptotic cells from oncotic cells. AnnexinV-FITC and PI double staining results showed that the apoptotic cells were rarely found in all groups, and the number of oncotic cells increased accompanied by an rise in the drug concentration. All these data suggested that ART induces gastric cancer cell death through oncosis, not apoptosis.

Calpain, especially calpain-2, is considered to be involved in oncosis-like cell death [20]. Calpains are a family of calcium-dependent cysteine proteases that perform limited proteolytic cleavage of a variety of cellular substrates [21]. Previous studies have indicated that calpain cleaves its target molecules, including spectrin, paxillin, and vinculin, inducing an oncotic phenotype [20,21]. Immunocytochemistry and western blot analysis confirmed a significant increase in calpain-2 expression in ART-treated cells compared with the negative control ones. Previous work has shown that the increased cytoplasmic concentration of free calcium ion leads to the activation of calpain [20,21]. In addition, Cummings *et al.* [22] reported that Ca^{2+} plays a key role in the mediation of cPLA2-mediated oncosis in renal cells. As shown in the results determined with Fluo-3/AM by flow cytometry, ART caused an increase in the cytosolic Ca^{2+} level in a dose-dependent manner. Therefore, calcium-mediated activation of calpain-2 may be involved in the oncosis-like cell death induced by ART.

Angiogenesis is an essential phenotype in growth and development [23], wound healing [24], and reproduction [25,26]. VEGF is commonly expressed in a wide variety of human tumor cells and has been associated with angiogenesis, growth, metastasis, and poor outcome in solid tumors [27]. In the present study, we verified

that VEGF, a key mediator of tumor angiogenesis, is inhibited by ART at the level of protein from cultured BGC-823 cells. Our findings are consistent with those reported previously, whereby ART can suppress angiogenesis and downregulate VEGF expression [28,29] to exert its anticancer effect. Previous studies have shown that energy depletion caused by the lack of angiogenesis will cause a breakdown of ion homeostasis, particularly of calcium [30]. In agreement with these observations, we found that the inhibition of VEGF secretion by ART was accompanied by an increase in the Ca^{2+} level in BGC-823 cells. Thus, it is plausible that downregulation of VEGF may be involved in ART-induced BGC-823 cell oncosis.

In conclusion, ART shows selective cytotoxic activity against human gastric cancer through oncosis-like cell death. The mechanisms may be associated with downregulation of VEGF and calcium-mediated activation of calpain-2. Further studies are required to understand the molecular mechanism of oncosis, which is a complex network composed of many factors.

Acknowledgements

This study was sponsored by a grant of the Foreign Cooperation Major Project of Wenzhou city (H20080056).

Conflicts of interest

There are no conflicts of interest.

References

1 Klayman DL. Qinghaosu (artemisinin): an antimalarial drug from China. *Science* 1985; **228**:1049–1055.
2 Luo XD, Shen CC. The chemistry, pharmacology, and clinical applications of qinghaosu (artemisinin) and its derivatives. *Med Res Rev* 1987; **7**:29–52.
3 Adjuik M, Babiker A, Garner P, Olliaro P, Taylor W, White N. Artesunate combinations for treatment of malaria: meta-analysis. *Lancet* 2004; **363**:9.
4 Efferth T, Rucker G, Falkenberg M, Manns D, Olbrich A, Fabry U, *et al.* Detection of apoptosis in KG-1a leukemic cells treated with investigational drugs. *Arzneimittelforschung* 1996; **46**:196–200.
5 Efferth T, Dunstan H, Sauerbrey A, Miyachi H, Chitambar CR. The antimalarial artesunate is also active against cancer. *Int J Oncol* 2001; **18**: 767–773.
6 Efferth T, Sauerbrey A, Olbrich A, Gebhart E, Rauch P, Weber HO, *et al.* Molecular modes of action of artesunate in tumor cell lines. *Mol Pharmacol* 2003; **64**:382–394.
7 Xue-lian T. The oncosis and apoptosis-inducing effect of artesunate on the K562 human leukemia cell line. *J Chongqing Med Univ* 2008; **7**:011.
8 Du JH, Zhang HD, Ma ZJ, Ji KM. Artesunate induces oncosis-like cell death in vitro and has antitumor activity against pancreatic cancer xenografts in vivo. *Cancer Chemother Pharmacol* 2010; **65**:895–902.
9 Majno G, Joris I. Apoptosis, oncosis, and necrosis. An overview of cell death. *Am J Pathol* 1995; **146**:3–15.
10 Trump BE, Berezesky IK, Chang SH, Phelps PC. The pathways of cell death: oncosis, apoptosis, and necrosis. *Toxicol Pathol* 1997; **25**:82–88.
11 Van Cruchten S, Van Den Broeck W. Morphological and biochemical aspects of apoptosis, oncosis and necrosis. *Anat Histol Embryol* 2002; **31**:214–223.
12 Suzuki M, Harada S, Owaribe K, Yaoita H. Intracellular ionic changes induced by bullous pemphigoid IgG subclasses. *Autoimmunity* 1996; **23**:181–197.
13 Naito S, von Eschenbach AC, Giavazzi R, Fidler IJ. Growth and metastasis of tumor cells isolated from a human renal cell carcinoma implanted into different organs of nude mice. *Cancer Res* 1986; **46**:4109–4115.
14 Brush MD. Recourse to death. *The Scientist* 2000; **14**:25.
15 Kim HK, Choi IJ, Kim CG, Kim HS, Oshima A, Michalowski A, *et al.* A gene expression signature of acquired chemoresistance to cisplatin and fluorouracil combination chemotherapy in gastric cancer patients. *PLoS One* 2011; **6**:e16694.
16 Efferth T, Giaisi M, Merling A, Krammer PH, Li-Weber M. Artesunate induces ROS-mediated apoptosis in doxorubicin-resistant T leukemia cells. *PLoS One* 2007; **2**:e693.
17 Hou J, Wang D, Zhang R, Wang H. Experimental therapy of hepatoma with artemisinin and its derivatives: in vitro and in vivo activity, chemosensitization, and mechanisms of action. *Clin Cancer Res* 2008; **14**:5519–5530.
18 Michaelis M, Kleinschmidt MC, Barth S, Rothweiler F, Geiler J, Breitling R, *et al.* Anti-cancer effects of artesunate in a panel of chemoresistant neuroblastoma cell lines. *Biochem Pharmacol* 2010; **79**:130–136.
19 Xu Q, Li ZX, Peng HQ, Sun ZW, Cheng RL, Ye ZM, *et al.* Artesunate inhibits growth and induces apoptosis in human osteosarcoma HOS cell line in vitro and in vivo. *J Zhejiang Univ Sci B* 2011; **12**:247–255.
20 Liu X, Van Vleet T, Schnellmann RG. The role of calpain in oncotic cell death. *Annu Rev Pharmacol Toxicol* 2004; **44**:349–370.
21 Goll DE, Thompson VF, Li H, Wei W, CONG J. The calpain system. *Physiol Rev* 2003; **83**:731–801.
22 Cummings BS, McHowat J, Schnellmann RG. Phospholipase A2s in cell injury and death. *J Pharmacol Exp Ther* 2000; **294**:793–799.
23 Risau W, Drexler H, Mironov V, Smits A, Siegbahn A, Funa K, *et al.* Platelet-derived growth factor is angiogenic in vivo. *Growth Factors* 1992; **7**:261–266.
24 Arnold F, West DC. Angiogenesis in wound healing. *Pharmacol Ther* 1991; **52**:407–422.
25 Welsh AO, Enders AC. Chorioallantoic placenta formation in the rat: II. Angiogenesis and maternal blood circulation in the mesometrial region of the implantation chamber prior to placenta formation. *Am J Anat* 1991; **192**:347–365.
26 Rogers P, Abberton K, Susil B. Endothelial cell migratory signal produced by human endometrium during the menstrual cycle. *Hum Reprod* 1992; **7**:1061–1966.
27 Ferrara N, Davis-Smyth T. The biology of vascular endothelial growth factor. *Endocr Rev* 1997; **18**:4–25.
28 Dell'Eva R, Pfeffer U, Vene R, Anfosso L, Forlani A, Albini A, *et al.* Inhibition of angiogenesis in vivo and growth of Kaposi's sarcoma xenograft tumors by the anti-malarial artesunate. *Biochem Pharmacol* 2004; **68**:2359–2366.
29 Zhou HJ, Wang WQ, Wu GD, Lee J, Li A. Artesunate inhibits angiogenesis and downregulates vascular endothelial growth factor expression in chronic myeloid leukemia K562 cells. *Vascul Pharmacol* 2007; **47**:131–138.
30 Siesjö B. Calcium and ischemic brain damage. *Eur Neurol* 2008; **25**:45–56.